

ORIGINAL PAPER



Experimental model for the study of traumatic brain injury

ILIE DUMITRU¹⁾, MARIAN VALENTIN ZORILĂ²⁾, RĂZVAN ȘTEFAN ȚOLESCU³⁾, LAURENȚIU RACILĂ⁴⁾, CRISTINA ÎLEANA PASCU¹⁾, ALEXANDRU CONSTANTIN OPRICA⁵⁾, DANIELA VASILICA BURGHILĂ⁶⁾, LUCIAN MATEI¹⁾, ELENA JANINA VÎLCEA⁷⁾, CRISTINA POPESCU⁸⁾, OANA BADEA-VOICULESCU⁹⁾, LAURENȚIU MOGOANTĂ¹⁰⁾

¹⁾Department of Road Vehicles and Transportation, Faculty of Mechanics, University of Craiova, Romania

²⁾Department of Forensic Medicine, University of Medicine and Pharmacy of Craiova, Romania

³⁾PhD Student, Department of Histology, University of Medicine and Pharmacy of Craiova, Romania

⁴⁾Department of Applied Mechanics, Faculty of Mechanics, University of Craiova, Romania

⁵⁾PhD Student, Department of Road Vehicles and Transportation, University of Craiova, Romania

⁶⁾University of Agronomic Sciences and Veterinary Medicine of Bucharest, Romania

⁷⁾Department of Manufacturing Engineering, Politehnica University of Bucharest, Romania

⁸⁾Department of Anatomy and Embryology, University of Medicine and Pharmacy of Craiova, Romania

⁹⁾Department of Modern Languages, University of Medicine and Pharmacy of Craiova, Romania

¹⁰⁾Research Center for Microscopic Morphology and Immunology, University of Medicine and Pharmacy of Craiova, Romania

Abstract

Traumatic brain injury (TBI) represents a public healthcare problem and a major economic burden, all over the world. It is estimated that every year, on the globe, there occur about two million severe TBI and over 42 million mild TBI. The main causes of TBI in civil population are fallings, followed by car accidents. In the last decades, the accelerated development of car industry and the poor development of traffic infrastructure in low- and average-income countries led to an increasing number of brain injuries, this becoming a major problem for medical health systems. According to some studies, approximately 1.35 million people die every year because of car accidents. In the last four decades, these types of injuries started to be studied in order to understand the lesion mechanisms for developing new safety equipment that may be installed on vehicles. The device presented by us for causing a TBI in a lab rat (mechanical pendulum) allows the performance of several major types of TBI, according to the kinetic energy, exposure area, contact surface, etc. The impact energies obtained by the device we presented may vary on a large scale, from less than 1 J up to 10 J, according to its weight, launching angle and impact head shape, thus being obtained minor, moderate or severe TBI.

Keywords: traumatic brain injury, mortality, brain contusions, experimental model, pathophysiology, neurologic deficits.

Introduction

Traumatic brain injury (TBI) represents a public healthcare problem and a major economic burden at worldwide level. The exact number of TBIs is not known all over the world, because some brain injuries considered “minor” do not require medical care or the healthcare systems in many countries do not have high standards, they do not record and do not report properly the number of TBI. However, some studies state that, every year, worldwide, over two million people undergo a severe [1] and over 42 million people undergo mild TBIs (mTBIs), clinically called concussion [2, 3]. Only in the US there is estimated that every year there occur about 1.6–3.8 million mTBIs [4, 5].

There should be emphasized that most persons suffering from a concussion undergo a full recovery in a few weeks’ time, but a significant number of these patients will present chronic brain dysfunction and disability, such as: headaches, dizziness, behavior changes, memory disturbance, motor deficiency, insomnia, mental disorders, etc. [6, 7].

Most studies show that the basic lesion mechanisms causing these pathological states remain unclear and require further research [3, 8].

The costs for the care of TBI patients are tremendous. Only in the US there is estimated a total cost for TBI (direct costs of medical treatment and death, as well as the impact on the production activity) of about 60.43 billion dollars [9].

The main causes for TBI in general population are fallings, followed by car accidents [10]. Both in developed countries and in the developing ones, car accidents represent one of the main causes of severe TBI, especially in the young, followed by death or survival with disabilities, more or less severe [1]. In a report, the *World Health Organization* (WHO) stated that in 2012 there were recorded about 1 255 000 deaths caused by car accidents all over the world. The rate of accidents increased constantly, by 0.3% between 2000 and 2012, despite the efforts made by most states of the world regarding a higher quality of the roads and the traffic legislation. Due to these reasons,

WHO considers that car accidents is, and will be, a main cause of death. Every year, worldwide, there are injured about 30–50 million people, and the expenses related to car accidents raise up to 1–2% of the gross domestic product (GDP) [11].

Aim

In order to correlate the intensity of the TBI to the severity of brain lesions, we created a mechanic device and experimental model, which reproduces various types of TBI in the laboratory animal (rats) from the mildest to the most severe ones.

Materials and Methods

The paper aims in creating a special device that can be used for studying TBI on lab rats, based on different blunt forced traumas created by different hitting impact energies. These energies are created by different types of object that are hitting the skull of the laboratory animals (rats).

The authors designed and made a dedicated device, with large customization capabilities. Thus, based on the calculations, a device with a pendulum type was designed, modeled, and calibrated.

Our device made for TBI production is composed of two lateral portal structures, necessary for the support of the pendulum and rigidity of the structure (Figure 1).

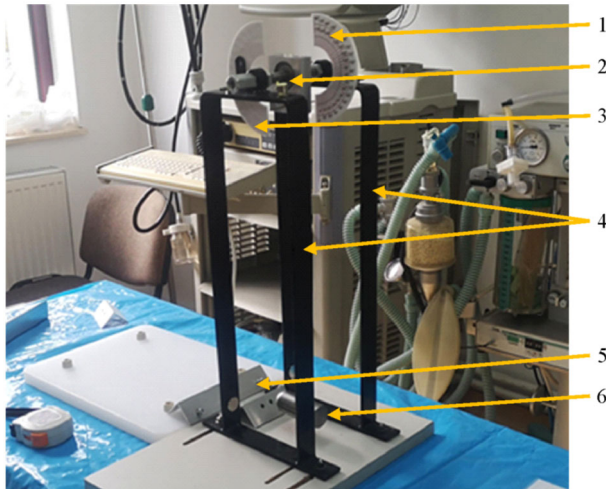


Figure 1 – Pendulum-type device for TBI production. 1: Graded angular quadrant for measuring the launching angle; 2: System for supporting the axis, spindle and impact head (element), equipped with a rolling lag; 3: Graded angular quadrant for measuring the comeback angle; 4: Portal supporting structure; 5: Support and positioning systems for the lab rat; 6: Impact head. TBI: Traumatic brain injury.

The materials used for the portal-type structure are general use laminated unalloyed steel, used in metallic constructions, with the S235JR symbol, with a draining limit $R_c = 235$ MPa. The impact heads (elements) of the device were made from carbonated steel of C45 type, having a draining limit $R_c = 480$ MPa. This type of steel is used in car manufacture industry, with high resistance and average tenacity, used for average and strong stressed pieces, having a good resistance to shocks (resilience $KCU = 60$ J/cm²), being an ideal solution from a qualitative

point of view for the impact head. Because this type of steel is difficult to solder, there was chosen the use of the spindle and impact head, threaded, preserving the measures imposed for the device design. As it may be observed in our images (Figures 2 and 3), the impact head may have different shapes, sizes, weights, and impact surfaces (round, oval or pointed) that allow the experimental reproduction of some various TBIs, including of some penetrating TBIs (pTBIs).

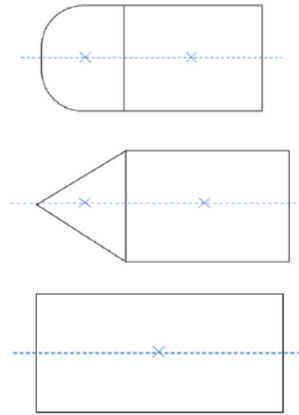


Figure 2 – Types of heads used in the generation of the TBI. TBI: Traumatic brain injury.

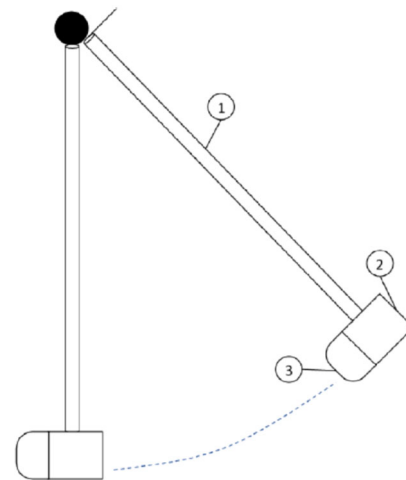


Figure 3 – Pendulum device used for TBI. 1: Pendulum rod; 2 and 3: Impact base and head. TBI: Traumatic brain injury.

The device is equipped with two angular quadrants for measuring the launching angle and the subsequent lifting angle after the impact, also having an indicator for determining these angles.

This type of device was thought and designed for obtaining impact energies that satisfy a large area of energies necessary to produce TBI specific lesions.

Results

Design of the TBI device

Kinetic energy calculation

The impact energy between the impact head and the rat is a kinetic energy, considering the entire assembly as a rigid solid in rotating motion around a fixed axis, where this axis passes through the center of the bearing.

Based on the assumption described above for a solid moving solid, kinetic energy can be written as:

$$E_C = \frac{1}{2} \cdot m \cdot v_0^2 + m(\vec{v}_0, \vec{\omega}, \vec{r}_0) + \frac{1}{2} \vec{\omega} [\vec{J} \vec{\omega}] \quad (1)$$

In the above expression, m is the mass of the rigid solid assembly (RSA), v_0 is the linear speed, ω is the angular velocity and J is the matrix attached to the inertia tensor of the RSA.

In the particular case of a rigid solid that is rotating about an axis Δ , the expression of kinetic energy is simplified and so it becomes:

$$E_C = \frac{1}{2} * \omega \vec{l} [\vec{J}_0 * (\omega \vec{l})] = \frac{1}{2} * J_{xx} * \omega^2 = \frac{1}{2} * J_{\Delta} * \omega^2 \quad (2)$$

Where ω is the angular velocity of the RSA and J_{Δ} is the moment of inertia of the RSA in relation to the axis of rotation.

Theoretical calculation of the device – moment of inertia

The device used for the creation of TBI in lab rats was created based on the pendulum movement of a weight with different impact tips, round, arrow or hemisphere (Figure 2).

The moment of inertia of the RSA relative to the axis of rotation is determined by considering that the pendulum consists of three RSAs. For each of these RSAs, the moment of inertia will be determined with respect to its own central axis system (passing through the center of its own weight). Applying Steiner–Huygens relation translates these moments of inertia to the axis of rotation of the

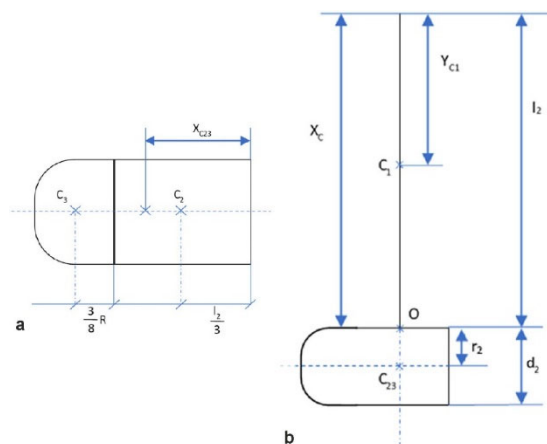


Figure 4 – (a and b) Weight center points and positioning in the rigid solid assembly (RSA).

Based on the 3D construction of the pendulum, we were able to analyze different types of impact heads structures and weight. At the same time, due to initial calibration of the pendulum with different types of heads, we established a range of kinetic energies that the pendulum can develop in different instances.

Following the different pendulum models evaluation through the construction and 3D analysis in with finite element method, the next stage started, that was the construction of the experimental pendulum model that can be seen in the Figure 6 (a and b).

The experimental model of the pendulum was used to cause trauma by hitting the skull of laboratory rats. In order to be able to evaluate the energies that compose the

pendulum, the moment of final inertia being the sum of the three moments of inertia.

The first step is to determine the coordinate’s weight center of the pendulum, by determining weight center of each RSA that makes up the pendulum. Also, the rod is screwed in the weight center of the impact base body (Figure 4, a and b).

The coordinates of the weight center points are:

$$x_{C23} := \frac{x_{C2} \cdot V_2 + x_{C3} \cdot V_3}{V_2 + V_3} = 35.08929 \text{ mm} \quad (3)$$

$$y_C := \frac{y_{C1} \cdot V_1 + y_{C23} \cdot V_{23}}{V_1 + V_{23}} = 400.29871 \text{ mm} \quad (4)$$

After the above calculation, it can be seen that the weight center is y_C and it is at 400.29871 mm from the rotation axis. Since the axis of rotation is considered the axis of Ox , only the moments in relation to this axis are considered. These moments are translated between own weight center and the axis of rotation of the whole pendulum, using the Steiner–Huygens relation, and the moment of inertia for the whole pendulum is:

$$J_{\Delta} = 68497963.34066 \text{ gm} \cdot \text{mm}^2 \quad (5)$$

Calculation of the device – kinetic energy

Following the impact calculations, we developed a three-dimensional (3D) model of a pendulum which we tested and analyzed through multiple software. The 3D reconstruction of the device can be seen in Figure 5 (a–c).

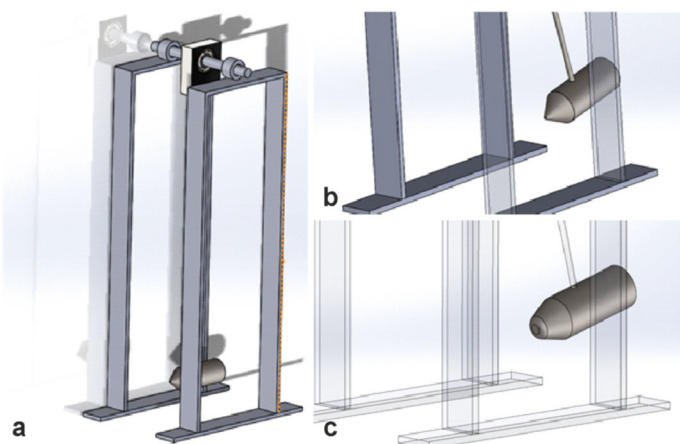


Figure 5 – (a–c) 3D analysis of the pendulum with different type of penetrators with Solid WORKS. 3D: Three-dimensional.

frontal impact as well as possible and for each test subject to be evaluated with the procedure, a process was developed and can be seen in the diagram below (Figure 7).

The first experiments we conducted with the pendulum evaluated the state of freedom of the lab rat with regards to the degree of freedom after the impact. The first impact of the lab rat was done with the rat without constrain and so the kinetic energy of the impact was very low (Figure 8, a–c).

In the next experiments, we introduced an element for the head positioning, so that the impact should be perpendicular to the lab rat head and the impact energy delivered to the skull trough the impact it will be much higher.

Starting from the algorithm presented above and based on the calibration of the experiments explained above, the following are determined:

- The distance measured (in relation to the reference plane system) before impact, using the “last frame” method, $d=11.5$ mm;
- The impact velocity was calculated $v = f \cdot d = 2.76$ m/s, having as input data the distance and the recording video frame rate, $f=240$ fps;
- Calculation of angular velocity, $\omega = v/v_c = 6.89$ s⁻¹.

Based on the above, the kinetic energy can be calculated at the moment of impact:

$$E_C := \frac{1}{2} \cdot J_{\Delta} \cdot \omega^2 = 1.62816 \frac{kg \cdot m^2}{s^2} \quad (6)$$

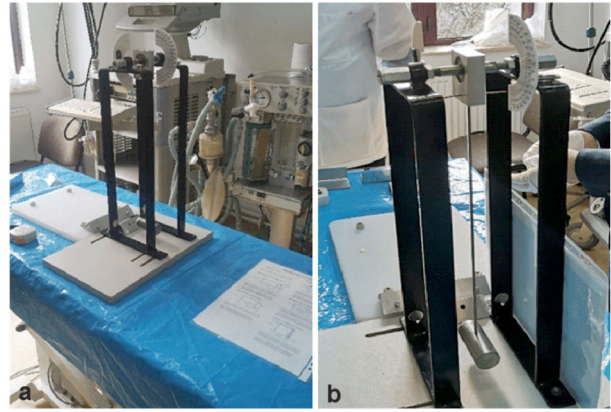


Figure 6 – (a and b) The experimental model of the pendulum.

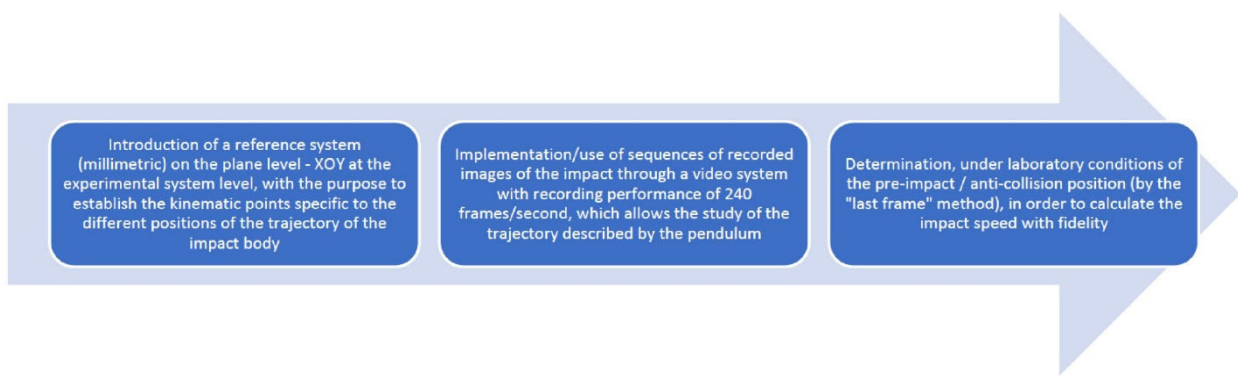


Figure 7 – Steps in laboratory experiments.

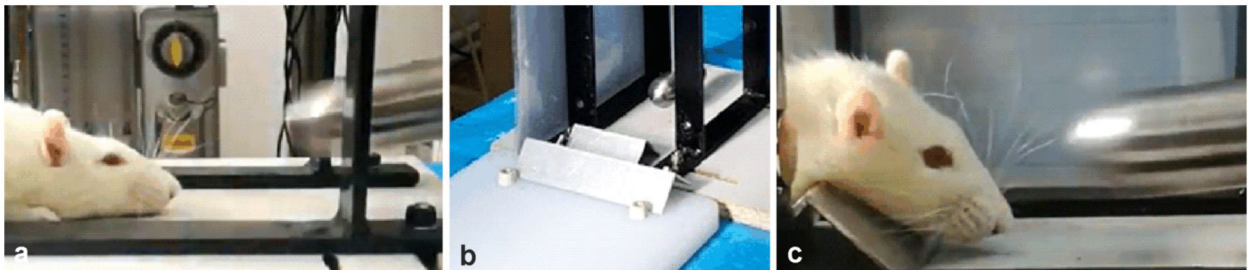


Figure 8 – Initial calibration of the pendulum: (a) First calibration experiment; (b) Head positioning element; (c) Second experiment of the rat skull hit.

Experimental calculation

Calculation of the device – impact energy

In order to calculate the real impact energy, *i.e.*, the energy transferred as a result of the impact in the contact area of the lab rat’s skull (mouse/lab rat), it is necessary to determine the lost energy.

The energy lost because of the impact was calculated in relation to β angle, described by the axis of the active assembly, in the direction of the movement. This angle was determined from the filming of the skull hits, using the “last frame” method.

Considering the deviation of the values of β angle can calculate between 0° and 90°, the energy lost by impact obtaining values between 0 J and 1.64 J:

$$E_{pier} := masa_{tot} \cdot g \cdot y_C \cdot (1 - \cos(\beta)) = \begin{bmatrix} 0 \\ 0.02481 \\ 0.09848 \\ 0.21879 \\ 0.38206 \\ 0.58334 \\ 0.81652 \\ 1.07451 \\ 1.34947 \\ 1.63305 \end{bmatrix} \frac{kg \cdot m^2}{s^2} \quad (7)$$

Based on the lost energy, it was possible to calculate the impact energy, which the skull absorbs after the blow (Figure 9):

$$E_{pier} := masa_{tot} \cdot g \cdot y_C \cdot (1 - \cos(\beta)) \quad (8)$$

$$E_{pier} = \begin{bmatrix} 0 \\ 0.02481 \\ 0.09848 \\ 0.21879 \\ 0.38206 \\ 0.58334 \\ 0.81652 \\ 1.07451 \\ 1.34947 \\ 1.63305 \end{bmatrix} \frac{kg \cdot m^2}{s^2} \quad (9)$$

Another way to calculate the impact energy was to enter the α and β angles corresponding to the position of the pendulum before and after the impact in the calculation of the equation. Thus, the graph was generated both for the 3D curve of the impact energy and for the energy distribution according to angles:

$$E_{impact_{i,j}} \leftarrow \frac{J_{\Delta}}{2} \cdot 2 \cdot g \cdot \frac{(1 - \cos(\alpha_{i,0}))}{y_C} - m \cdot a_{tot} \cdot g \cdot y_C \cdot (1 - \cos(\beta_{j,0})) \quad (10)$$

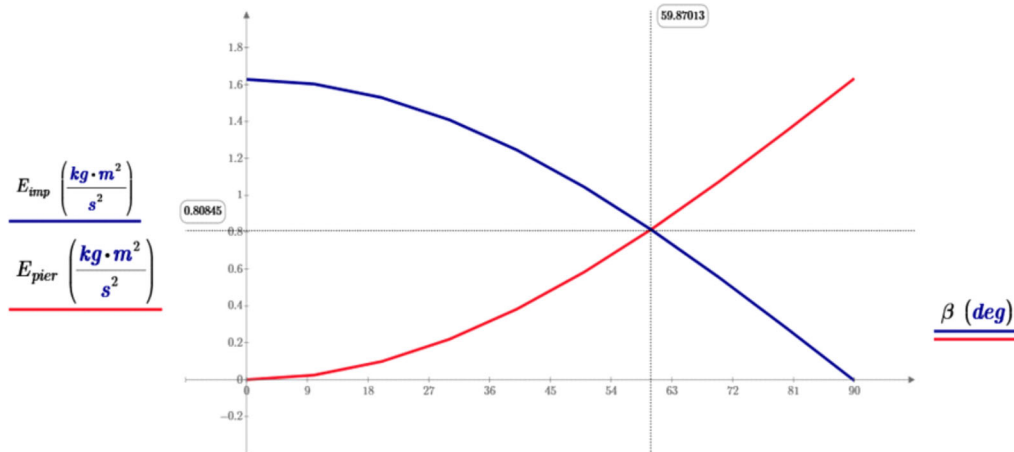


Figure 9 – Impact energy related to lost energy.

Because the equation considers the α and β angles, the actual calculation was performed by the calculation

algorithms, presented below:

$$E_{fin} := \text{for } i \in 0.. \text{rows}(\alpha) - 1 \quad \left\| \begin{array}{l} \text{for } j \in 0.. \text{rows}(\beta) - 1 \\ E_{impact_{i,j}} \leftarrow \frac{J_{\Delta}}{2} \cdot 2 \cdot g \cdot \frac{(1 - \cos(\alpha_{i,0}))}{y_C} - m \cdot a_{tot} \cdot g \cdot y_C \cdot (1 - \cos(\beta_{j,0})) \\ \text{if } E_{impact_{i,j}} < 0 \\ \quad \left\| \begin{array}{l} E_{impact_{i,j}} \leftarrow 0 \\ E_{impact} \end{array} \right\| \end{array} \right\| \quad (11)$$

As can be seen, the energy formula was calculated at each β angle for each α angle, and the graphical results

can be seen in the equation below. Calculations are made for the angular deviation between 0–180°:

$$E_{fin} = \begin{bmatrix} 0.09008 & 0.11489 & 0.18857 & 0.30887 & 0.47214 & 0.67343 & 0.9066 & 1.16459 & 1.43955 & 1.72313 \\ 0.06459 & 0.0894 & 0.16307 & 0.28337 & 0.44665 & 0.64793 & 0.88111 & 1.1391 & 1.41406 & 1.69763 \\ 0 & 0.01369 & 0.08736 & 0.20767 & 0.37094 & 0.57222 & 0.8054 & 1.06339 & 1.33835 & 1.62193 \\ 0 & 0 & 0 & 0.08405 & 0.24732 & 0.4486 & 0.68178 & 0.93977 & 1.21473 & 1.49831 \\ 0 & 0 & 0 & 0 & 0.07954 & 0.28083 & 0.51401 & 0.77199 & 1.04695 & 1.33053 \\ 0 & 0 & 0 & 0 & 0 & 0.07399 & 0.30717 & 0.56516 & 0.84012 & 1.12369 \\ 0 & 0 & 0 & 0 & 0 & 0 & 0.06756 & 0.32555 & 0.60051 & 0.88408 \\ 0 & 0 & 0 & 0 & 0 & 0 & 0 & 0.06045 & 0.3354 & 0.61898 \\ 0 & 0 & 0 & 0 & 0 & 0 & 0 & 0 & 0.05286 & 0.33644 \\ 0 & 0 & 0 & 0 & 0 & 0 & 0 & 0 & 0 & 0.04504 \\ 0 & 0 & 0 & 0 & 0 & 0 & 0 & 0 & 0 & 0 \\ 0 & 0 & 0 & 0 & 0 & 0 & 0 & 0 & 0 & 0 \end{bmatrix} \frac{kg \cdot m^2}{s^2} \quad (12)$$

Based on the result matrix above, the spatial graph of the impact energy can be realized (Figure 10, a and b).

At the same time, the energy contour graph was evaluated according to the α and β angles (Figure 11).

The device model presented is a mechanic pendulum type, the subject lab rat being in a free state, with the body not fixed. For evaluating the impact energy there was calculated the energy before impact, the speed at impact and the energy after the impact, being performed a theoretical

and experimental calculus. The evaluation of energy after impact may also be performed by estimating the movement of the solitary placed lab rat in a moving cart on the device table, the mechanic and friction characteristics between the table and the cart. In order to maximize the energy transferred after the impact between the impact head and the lab rat, there may be used a fixing tank device with the pendulum device table.

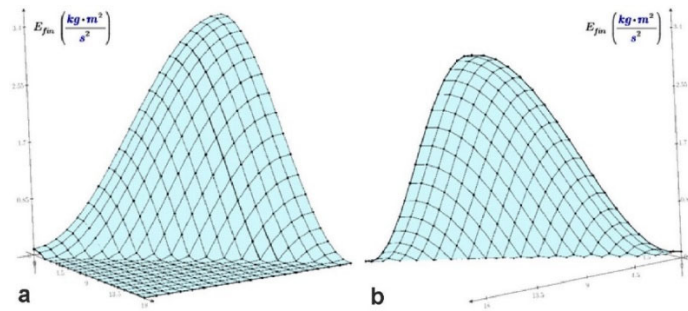


Figure 10 – (a and b) The spatial graph based on the α and β angles.

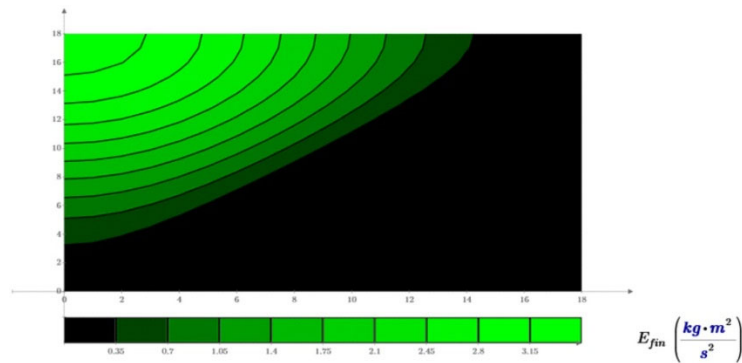


Figure 11 – The contour graph according to the α and β angles.

Preliminary histological study

The study was approved by the Ethics Committee of the University of Medicine and Pharmacy of Craiova, Romania. The study was performed on a small number of laboratory animals (five rats) to verify the ability of the device created by us to produce specific TBIs. We used five adult rats, common Wistar breed, weighing 350–370 g, which were kept in the Animal Facility of the University of Medicine and Pharmacy of Craiova, in optimal conditions of light and humidity, with free access to food and water, which were monitored both before and after the experiment. Animals were anesthetized before trauma with Ketamine (Ketalar[®]) 85 mg/kg body weight (b.w.) and Xylazine (Rompun[®]) 6 mg/kg b.w., and received a single shot of 5 J.

Forty-eight hours after the application of the trauma,

the animals were sacrificed, the brain was completely harvested, fixed in 10% neutral buffered formalin solution, and included in paraffin according to the classical histological technique. At the microtome, sections of 4 μ m were made, which were stained with Hematoxylin–Eosin (HE).

The microscopic examination showed that the largest lesions of the nervous system tissue from the brain hemispheres were recorded in the frontal lobe, where the traumatic impact was maximum. Here, there could be observed the presence of some complex lesions that affected the neurons (incipient neuronal apoptosis), glial cells (glial moderate reaction – reactive gliosis), blood vessels (vascular congestion, perivascular hemorrhages in the Virchow–Robin spaces, multiple diffuse, intraparenchymal hemorrhages) (Figures 12 and 13).

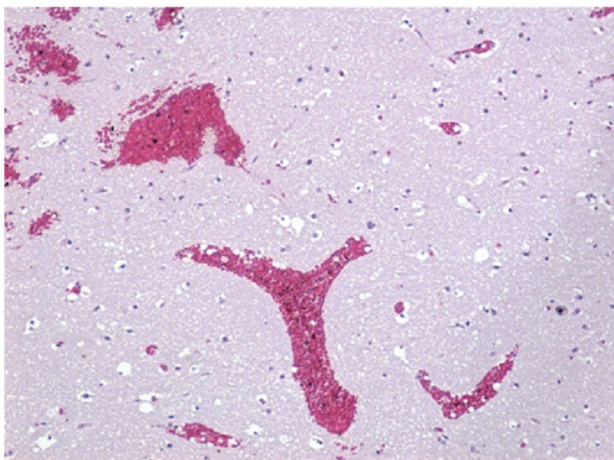


Figure 12 – Area of frontal lobe highlighting strongly congested blood vessels, perivascular hemorrhages in the Virchow–Robin spaces, diffuse intraparenchymal hemorrhages and incipient neuronal apoptosis (HE staining, $\times 40$).

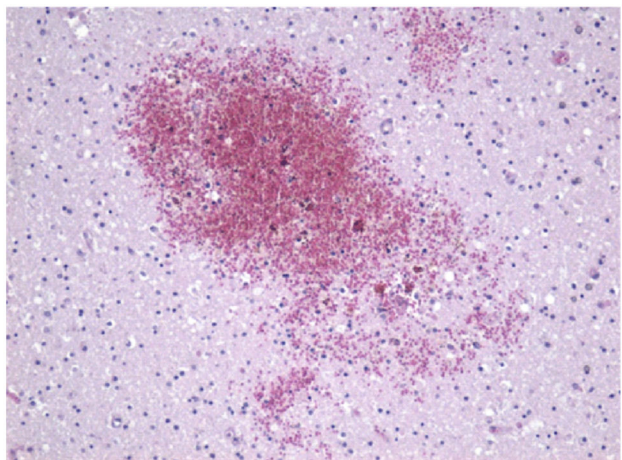


Figure 13 – Diffuse intraparenchymal hemorrhage in the frontal lobe (HE staining, $\times 100$).

In the white substance, there were observed diffuse demyelinations of the axons, vascular congestion, and perivascular edema. Similar phenomena, yet of lower

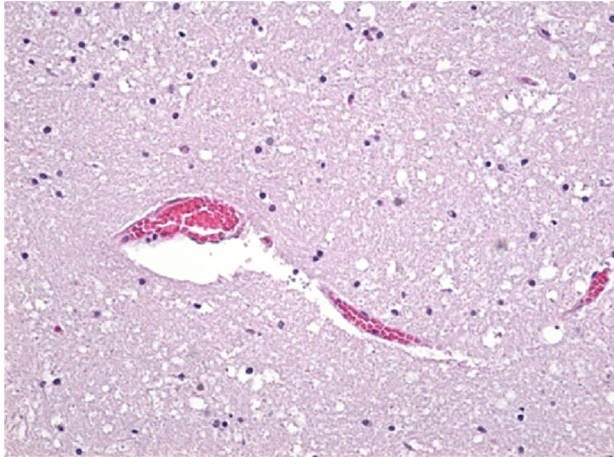


Figure 14 – Image of vascular congestion associated with perivascular edema and neuronal apoptosis in the temporal lobe (HE staining, $\times 100$).

intensity and on less extended areas were also observed in the temporal or occipital lobes (Figures 14 and 15).

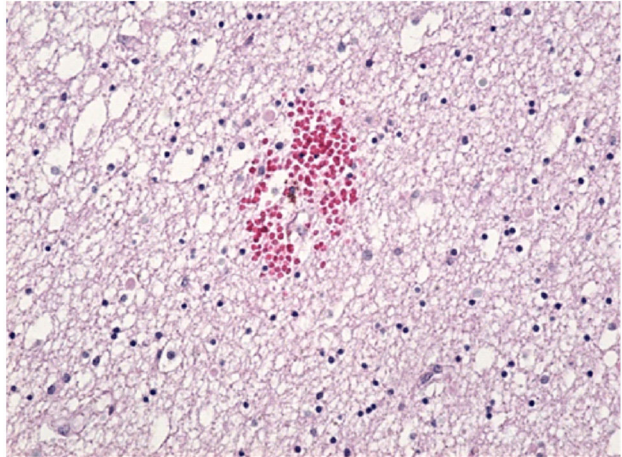


Figure 15 – Image of microhemorrhage in the white substance of the occipital lobe (HE staining, $\times 100$).

☒ Discussions

TBI represents a pathology that significantly contributes to the increase of morbidity and mortality worldwide, both in adults and in children [12]. In the European Union, there are recorded over one million hospitalizations due to TBI [13, 14].

Clinically, TBI is classified according to severity, based on the Glasgow Coma Scale (GCS), in mild, moderate or severe TBI, being associated with rates of permanent disabilities of 10%, 60% and 100%, respectively, and with global mortality rates of 20–30% [15]. Still, the TBI prognosis is not always correlated with the GCS. For most of the patients with mild TBI, the symptoms undergo remission in a few days or weeks, but there were also recorded patients in whom some symptoms, such as cognitive deficits or memory loss, persisted for a few months [16–19]. Even a mild TBI can also increase the risk of a person to develop a depression disorder, neurovegetative diseases, post-traumatic epilepsy, etc. [20–22].

There should be observed, also, that there are studies showing that some children who underwent severe TBI recovered completely from a mental point of view [12].

All these data show that the factors influencing the results (positive or negative) after TBI are nor completely known. All the studies showed that TBI generate a complex tandem of physiopathological processes that result in structural lesions of the encephalon or functional deficits through direct mechanisms (primary lesions caused by the mechanical agent) or by indirect mechanisms (secondary lesions). Primary lesions are represented by neuronal and glial cell lesions, always associated with vascular lesions (increase of vascular permeability, intraparenchymal hemorrhages, subdural hematomas) that, in their turn, lead to the increase of intra cranial pressure, heart attack and brain edema [23, 24].

The secondary lesions occur after a period lasting from a few hours to a few days after the primary lesion and they are the result of a tandem of subsequent, metabolic, cellular, and molecular events, which lead in the end to

the increase of brain cell death, tissular, vascular and degenerative lesions [25, 26].

A frequent cause of TBI are car accidents. In the last decades, the accelerated development of car industry and the poor development of traffic infrastructure in low- and average-income countries led to an increasing number of brain injuries, this becoming a major problem for medical health systems. According to some recent studies [27], approximately 1.35 million people die every year because of car accidents. Also, the economic cost of car accidents is estimated to 1% of the GDP in low-income countries, 1.5% in average-income countries and 2% in high-income countries [27, 28].

At present, the therapeutic plans, and the prognosis for the patients with severe or moderate TBI are limited due to the heterogeneity of lesions and the limited understanding of these lesions' physiopathology. In order to understand the physiopathology and histopathological changes of the brain in the TBI mainly caused by car accidents, we elaborated an experimental model that may be applied on lab rats.

It is well-known the fact that brain injuries resulted from the collision with a moving vehicle are correlated with its mechanic force that, in turn, depends on its speed and mass, but also on the contact surface with the human or animal body. The most frequent car accidents that cause TBI are the collision between two moving vehicles, the collision between a vehicle and an obstacle or between a vehicle and a pedestrian. In the last four decades, these types of injuries started to be studied in order to understand the lesional mechanisms for developing new safety equipment that may be installed on vehicles. For this, there were proposed several experimental injury models that may be applied on the lab rat, causing the physiopathological mechanism found in TBI in humans.

For obtaining a TBI, there were conceived and used several types of devices: pneumatic, electromagnetic, mechanic ones (by free falling, arch, projectile, etc.) [3, 14].

Our model, the mechanical pendulum, allows the performance of an important number of TBI on the lab rat, varying in kinetic energy, exposure area, contact surface, etc. The impact energies obtained by the device presented in this study may vary on a large scale, from less than 1 J up to over 10 J, according to its weight, launching angle and impact head shape, thus obtaining minor, moderate or severe TBI; it may cause focal lesions, even penetrant injuries, when the impact surface is small, or it may cause diffuse lesions when the impact surface with the animal head is large. It is a simple, easy to use system that allows the calculation of the device kinetic energy at the impact surface. Also, it may be applied for various types of TBI; it allows the fixation of the lab rat head or, on the contrary, it allows the free holding of the rat, including the introduction of some elastic devices that can buffer the impact, devices that imitate the “airbags” on the vehicles.

The presented device is a versatile one, which, besides the TBI production, may be used for the performance of bone fractures in lab rats, on different segments of the skeleton. For this type of experiments, the device is equipped with adjustable rigid tanks, therefore there may be adjusted both the tank height and the width between the two tank openings, for experiments including various types of bones.

Our model allows the control of the impact kinetic energy on the lab rat, it allows the performance of measurable lesions, identical with the ones present in humans with TBI, it allows the calculation of the impact energy and the anticipation of the brain injury severity, being also reproducible.

The preliminary histopathological study performed showed that the lesions made with the device presented by us in the encephalon are superior or, at least, identical with the lesions performed by other models, proposed by other authors [19, 24, 29–34].

☒ Conclusions

The device designed by us and used for TBI is a module device that may also be used for other types of experiments related to collisions (injuries/fractures). The solutions of the demountable assemblance penetrating head-spindle-support system may lead to a high versatility of the device, thus allowing the performance of various experiments according to the geometrical shape of the penetrating head, its mass, types of used tanks, their capacity of controlled movement or fixation, duration, variation speed and the amplitude of kinematic sizes. Also, according to the position of the lab rat, there may be performed direct frontal, lateral, superior, etc., TBIs. The impact energy may vary from subdivisions of 1 J up to 10 J, according to the impact head surface and its launching angle, the device being able to produce a multitude of TBI types, from mild forms to severe TBI or even pTBIs. As the complexity of the performed experiments increases, the device may be modified for a constructive-functional optimization, a future approach of collisions requiring its adjustment to the freedom degrees of subjects, as well as their kinematic and dynamic evolution after collision.

Conflict of interests

The authors declare that they have no conflict of interests.

Acknowledgments

This work was supported by the grant POCU380/6/13/123990, co-financed by the European Social Fund within the Sectorial Operational Program Human Capital 2014–2020.

References

- [1] Praveen Rajneesh C, Yang LY, Chen SC, Hsieh TH, Chin HY, Peng CW. Cystometric measurements in rats with an experimentally induced traumatic brain injury and voiding dysfunction: a time-course study. *Brain Sci*, 2019, 9(11):325. <https://doi.org/10.3390/brainsci9110325> PMID: 31739594 PMCID: PMC6895874
- [2] Gardner RC, Yaffe K. Epidemiology of mild traumatic brain injury and neurodegenerative disease. *Mol Cell Neurosci*, 2015, 66(Pt B):75–80. <https://doi.org/10.1016/j.mcn.2015.03.001> PMID: 25748121 PMCID: PMC4461453
- [3] Hoogenboom WS, Rubin TG, Ye K, Cui MH, Branch KC, Liu J, Branch CA, Lipton ML. Diffusion tensor imaging of the evolving response to mild traumatic brain injury in rats. *J Exp Neurosci*, 2019, 13:1179069519858627. <https://doi.org/10.1177/1179069519858627> PMID: 31308735 PMCID: PMC6613065
- [4] National Center for Injury Prevention and Control. Report to Congress on mild traumatic brain injury in the United States: steps to prevent a serious public health problem. Centers for Disease Control and Prevention (CDC), Atlanta, GA, USA, 2003. <https://www.cdc.gov/traumaticbraininjury/pdf/mtbireport-a.pdf>
- [5] Bodnar CN, Roberts KN, Higgins EK, Bachstetter AD. A systematic review of closed head injury models of mild traumatic brain injury in mice and rats. *J Neurotrauma*, 2019, 36(11):1683–1706. <https://doi.org/10.1089/neu.2018.6127> PMID: 30661454 PMCID: PMC6555186
- [6] Rosenbaum SB, Lipton ML. Embracing chaos: the scope and importance of clinical and pathological heterogeneity in mTBI. *Brain Imaging Behav*, 2012, 6(2):255–282. <https://doi.org/10.1007/s11682-012-9162-7> PMID: 22549452
- [7] Mayer AR, Quinn DK, Master CL. The spectrum of mild traumatic brain injury: a review. *Neurology*, 2017, 89(6):623–632. <https://doi.org/10.1212/WNL.0000000000004214> PMID: 28701496 PMCID: PMC5562956
- [8] Lo C, Shifteh K, Gold T, Bello JA, Lipton ML. Diffusion tensor imaging abnormalities in patients with mild traumatic brain injury and neurocognitive impairment. *J Comput Assist Tomogr*, 2009, 33(2):293–297. <https://doi.org/10.1097/RCT.0b013e31817579d1> PMID: 19346863
- [9] Bader M, Li Y, Tweedie D, Shlobin NA, Bernstein A, Rubovitch V, Tovar-Y-Romo LB, DiMarchi RD, Hoffer BJ, Greig NH, Pick CG. Neuroprotective effects and treatment potential of icretin mimetics in a murine model of mild traumatic brain injury. *Front Cell Dev Biol*, 2020, 7:356. <https://doi.org/10.3389/fcell.2019.00356> PMID: 31998717 PMCID: PMC6965031
- [10] Faul M, Xu L, Wald MM, Coronado VG. Traumatic brain injury in the United States: emergency department visits, hospitalizations, and deaths 2002–2006. U.S. Department of Health and Human Services, Centers for Disease Control and Prevention (CDC), National Center for Injury Prevention and Control, Division of Injury Response, Atlanta, GA, USA, March 2010. https://www.cdc.gov/traumaticbraininjury/pdf/blue_book.pdf
- [11] Ashraf I, Hur S, Shafiq M, Park Y. Catastrophic factors involved in road accidents: underlying causes and descriptive analysis. *PLoS One*, 2019, 14(10):e0223473. <https://doi.org/10.1371/journal.pone.0223473> PMID: 31596878 PMCID: PMC6785079
- [12] Holland JN, Schmidt AT. Static and dynamic factors promoting resilience following traumatic brain injury: a brief review. *Neural Plast*, 2015, 2015:902802. <https://doi.org/10.1155/2015/902802> PMID: 26347352 PMCID: PMC4539485
- [13] Hyder AA, Wunderlich CA, Puvanachandra P, Gururaj G, Kobusingye OC. The impact of traumatic brain injuries: a global perspective. *NeuroRehabilitation*, 2007, 22(5):341–353. <https://doi.org/10.3233/NRE-2007-22502> PMID: 18162698
- [14] Sempere L, Rodríguez-Rodríguez A, Boyero L, Egea-Guerrero JJ. Experimental models in traumatic brain injury: from animal models to *in vitro* assays. *Med Intensiva*, 2019, 43(6):362–372. <https://doi.org/10.1016/j.medin.2018.04.012> PMID: 30055817

- [15] Vella MA, Crandall ML, Patel MB. Acute management of traumatic brain injury. *Surg Clin North Am*, 2017, 97(5):1015–1030. <https://doi.org/10.1016/j.suc.2017.06.003> PMID: 28958355 PMID: PMC5747306
- [16] McAllister TW, Sparling MB, Flashman LA, Guerin SJ, Mamourian AC, Saykin AJ. Differential working memory load effects after mild traumatic brain injury. *Neuroimage*, 2001, 14(5):1004–1012. <https://doi.org/10.1006/nimg.2001.0899> PMID: 11697932
- [17] Dean PJA, Sterr A. Long-term effects of mild traumatic brain injury on cognitive performance. *Front Hum Neurosci*, 2013, 7:30. <https://doi.org/10.3389/fnhum.2013.00030> PMID: 23408228 PMID: PMC3569844
- [18] McMahan P, Hricik A, Yue JK, Puccio AM, Inoue T, Lingsma HF, Beers SR, Gordon WA, Valadka AB, Manley GT, Okonkwo DO; TRACK-TBI Investigators. Symptomatology and functional outcome in mild traumatic brain injury: results from the prospective TRACK-TBI study. *J Neurotrauma*, 2014, 31(1):26–33. <https://doi.org/10.1089/neu.2013.2984> PMID: 23952719 PMID: PMC3880097
- [19] Bolton-Hall AN, Hubbard WB, Saatman KE. Experimental designs for repeated mild traumatic brain injury: challenges and considerations. *J Neurotrauma*, 2019, 36(8):1203–1221. <https://doi.org/10.1089/neu.2018.6096> PMID: 30351225 PMID: PMC6479246
- [20] Holsinger T, Steffens DC, Phillips C, Helms MJ, Havlik RJ, Breitner JCS, Guralnik JM, Plassman BL. Head injury in early adulthood and the lifetime risk of depression. *Arch Gen Psychiatry*, 2002, 59(1):17–22. <https://doi.org/10.1001/archpsyc.59.1.17> PMID: 11779276
- [21] Plassman BL, Havlik RJ, Steffens DC, Helms MJ, Newman TN, Drosdick D, Phillips C, Gau BA, Welsh-Bohmer KA, Burke JR, Guralnik JM, Breitner JC. Documented head injury in early adulthood and risk of Alzheimer's disease and other dementias. *Neurology*, 2000, 55(8):1158–1166. <https://doi.org/10.1212/wnl.55.8.1158> PMID: 11071494
- [22] Catale C, Marique P, Closset A, Meulemans T. Attentional and executive functioning following mild traumatic brain injury in children using the Test for Attentional Performance (TAP) battery. *J Clin Exp Neuropsychol*, 2009, 31(3):331–338. <https://doi.org/10.1080/13803390802134616> PMID: 18608644
- [23] Gaetz M. The neurophysiology of brain injury. *Clin Neurophysiol*, 2004, 115(1):4–18. [https://doi.org/10.1016/s1388-2457\(03\)00258-x](https://doi.org/10.1016/s1388-2457(03)00258-x) PMID: 14706464
- [24] Cernak I. Animal models of head trauma. *NeuroRx*, 2005, 2(3):410–422. <https://doi.org/10.1602/neurorx.2.3.410> PMID: 16389305 PMID: PMC1144485
- [25] Bramlett HM, Dietrich WD. Progressive damage after brain and spinal cord injury: pathomechanisms and treatment strategies. *Prog Brain Res*, 2007, 161:125–141. [https://doi.org/10.1016/S0079-6123\(06\)61009-1](https://doi.org/10.1016/S0079-6123(06)61009-1) PMID: 17618974
- [26] Iboaya A, Harris JL, Arickx AN, Nudo RJ. Models of traumatic brain injury in aged animals: a clinical perspective. *Neuro-rehabil Neural Repair*, 2019, 33(12):975–988. <https://doi.org/10.1177/1545968319883879> PMID: 31722616 PMID: PMC6920554
- [27] Jalilian MM, Safarpour H, Bazayr J, Keykaleh MS, Malekyan L, Khorshidi A. Environmental related risk factors to road traffic accidents in Ilam, Iran. *Med Arch*, 2019, 73(3):169–172. <https://doi.org/10.5455/medarh.2019.73.169-172> PMID: 31402801 PMID: PMC6643320
- [28] World Health Organization (WHO). Global status report on road safety 2018. WHO, Geneva, 2018. <https://www.who.int/publications/i/item/9789241565684>
- [29] Longhi L, Saatman KE, Fujimoto S, Raghupathi R, Meaney DF, Davis J, McMillan BSA, Conte V, Laurer HL, Stein S, Stocchetti N, McIntosh TK. Temporal window of vulnerability to repetitive experimental concussive brain injury. *Neurosurgery*, 2005, 56(2):364–374; discussion 364–374. <https://doi.org/10.1227/01.neu.0000149008.73513.44> PMID: 15670384
- [30] Prieto R, Gutiérrez-González R, Pascual JM, Roda JM, Cerdán S, Matias-Guiu J, Barcia JA. Modelos experimentales de traumatismo craneoencefálico [Experimental models of traumatic brain injury]. *Neurocirugía (Astur)*, 2009, 20(3):225–244. PMID: 19575127
- [31] Cernak I. Blast-induced neurotrauma models and their requirements. *Front Neurol*, 2014, 5:128. <https://doi.org/10.3389/fneur.2014.00128> PMID: 25071713 PMID: PMC4091031
- [32] Sowers JL, Wu P, Zhang K, DeWitt DS, Prough DS. Proteomic changes in traumatic brain injury: experimental approaches. *Curr Opin Neurol*, 2018, 31(6):709–717. <https://doi.org/10.1097/WCO.0000000000000613> PMID: 30358641 PMID: PMC6221404
- [33] Kilbourne M, Kuehn R, Tosun C, Caridi J, Keledjian K, Bochicchio G, Scalea T, Gerzanich V, Simard JM. Novel model of frontal impact closed head injury in the rat. *J Neurotrauma*, 2009, 26(12):2233–2243. <https://doi.org/10.1089/neu.2009.0968> PMID: 19929375 PMID: PMC2824220
- [34] Delye H, Verschuere P, Depreitere B, Verpoest I, Berckmans D, Vander Sloten J, Van Der Perre G, Goffin J. Biomechanics of frontal skull fracture. *J Neurotrauma*, 2007, 24(10):1576–1586. <https://doi.org/10.1089/neu.2007.0283> PMID: 17970621

Corresponding author

Marian Valentin Zorilă, Assistant, MD, PhD, Department of Forensic Medicine, University of Medicine and Pharmacy of Craiova, 2 Petru Rareș Street, 200349 Craiova, Romania; Phone +40761–334 037, e-mail: zorilaval@yahoo.com.au

Received: October 15, 2020

Accepted: February 20, 2021